

# Constructing a Blue Light Photodetector on Inorganic/Organic p–n Heterojunction Nanowire Arrays

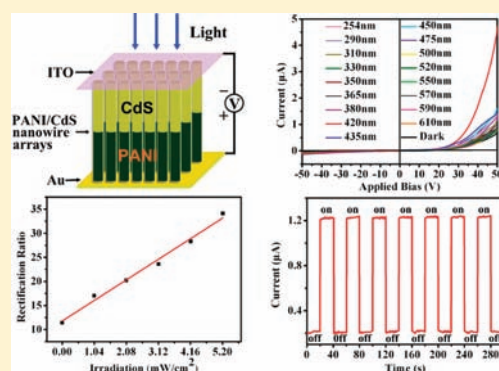
Haowei Lin,<sup>†</sup> Huibiao Liu,<sup>\*,†</sup> Xuemin Qian,<sup>†</sup> Siu-Wai Lai,<sup>‡</sup> Yongjun Li,<sup>†</sup> Nan Chen,<sup>†</sup> Canbin Ouyang,<sup>†</sup> Chi-Ming Che,<sup>‡</sup> and Yuliang Li<sup>\*,†</sup>

<sup>†</sup>The CAS Key Laboratory of Organic Solids, Beijing National Laboratory for Molecular Sciences (BNLMS), Institute of Chemistry, Chinese Academy of Sciences, Beijing 100190, P. R. China

<sup>‡</sup>Department of Chemistry and HKU-CAS Joint Laboratory on New Materials, The University of Hong Kong, Pokfulam Road, Hong Kong SAR, P. R. China

**S** Supporting Information

**ABSTRACT:** We described a new structure photodetector, which is constructed by p–n heterojunction nanowire arrays of PANI (polyaniline)/CdS. The nanowire arrays exhibit excellent rectifying features and a diode nature and show a sensitive spectral response to blue light under 420 nm. The rectification ratio plots of different illumination intensities show straight line behavior, implying that the quantitative detection of illumination intensity can be achieved. The p–n heterojunction nanowire array is a great candidate for applications in high-sensitivity and high-speed blue light photodetectors.



## INTRODUCTION

Recently, one-dimensional (1D) p–n heterojunction nanostructures have attracted particular attention because of their optical, optoelectronic, and electronic properties as well as their use as building blocks for highly sophisticated nanodevices.<sup>1–6</sup> One-dimensional p–n inorganic/organic heterojunction nanowires have demonstrated having excellent photovoltaic behavior, rectification, and light-emitting behavior.<sup>7–13</sup> The properties of these heterostructure materials are not only the sum of the individual contributions of both components but are also determined by processes that occur at the interfaces between the components. Either totally novel or improved physical and chemical properties might result from strong interaction between the organic and inorganic units, which aids in further understanding the organic–inorganic interface formed on the nanoscale and in fabricating novel nanoscale devices, and this offers great opportunities in both fundamental research and practical applications.

Recently, 1D nanostructures have been widely studied to enhance the quantum efficiency and shorten the response time of photodetectors. This approach originates from the large surface-to-volume ratio and low dimensionality in 1D nanostructure. Various low dimensional nanostructures of inorganic semiconductor materials (Si, GaN, GaAs, InP, InSe, ZnS, CdS, etc.) and semiconducting polymers have been used in photodetectors.<sup>14–28</sup> 1D nanostructures of inorganic semiconductor materials have been explored in depth; in general, GaN-, Si-, InGaAs-, and CdS-based

detectors are used for the three important sub-bands, 0.25–0.42  $\mu\text{m}$  (UV), 0.45–0.8  $\mu\text{m}$  (visible), and 0.9–1.7  $\mu\text{m}$  (NIR), respectively. However, most of them require a relatively long response time/decay time. Besides the inorganic semiconductor systems, semiconducting polymer photodetectors have undergone rapid development recently.<sup>16,18</sup> One-dimensional inorganic/organic p–n heterojunction nanostructures have exhibited highly photosensitive properties; nevertheless, there has been no report on the photodetectors based on p–n heterojunction nanowire arrays between organic and inorganic molecules. Herein, we report a novel system of inorganic/organic p–n heterojunction nanowire arrays for efficient photodetectors; the material exhibits excellent rectifying features and a diode nature. Importantly, the p–n heterojunction nanowire arrays show a highly sensitive spectral response and a significant response speed under blue light (420 nm); the rectification ratio plots of different illumination intensities show straight line behavior, implying that the quantitative detection of illumination intensity can be achieved. These excellent characterizations imply that the inorganic/organic semiconductor p–n heterojunction nanowire arrays are great candidates for applications on high-sensitivity and high-speed photodetectors and photoelectronic switches.

**Received:** April 28, 2011

**Published:** July 14, 2011

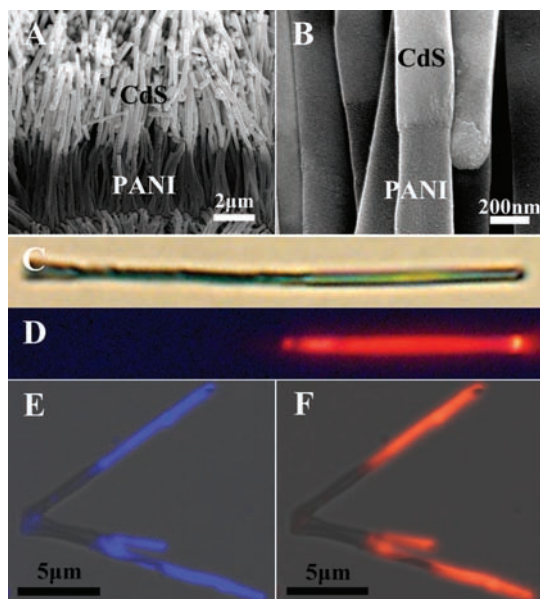


**Figure 1.** SEM images of PANI/CdS heterojunction nanowires. (A) Cross view of PANI/CdS nanowire arrays. (B) The p–n junctions of PANI/CdS heterojunction nanowires under a large-magnification. (C) Optional image of a single PANI/CdS heterojunction nanowire. (D) Fluorescent image of a single PANI/CdS heterojunction nanowire under excitation of 330–380 nm. (E) Fluorescent image of some typical PANI/CdS heterojunction nanowires ( $\lambda_{\text{ex}} = 405$  nm) collected from 470 to 520 nm. (F) Fluorescent image of some typical PANI/CdS heterojunction nanowires ( $\lambda_{\text{ex}} = 405$  nm) collected from 570 to 670 nm.

## EXPERIMENTAL SECTION

**Materials.** Aniline was purchased from Alfa Aesar Corporation. Sublimed sulfur, cadmium chloride, sulfuric acid, dimethyl sulfoxide (DMSO), acetonitrile, and acetone were purchased from Beijing Chemical Reagent Corporation, China. All of the reagents were used as received. The anodic aluminum oxide (AAO) templates with a porous diameter of 200 nm and a thickness of 60  $\mu\text{m}$  were purchased from Whatman Corporation. The nanowires were synthesized with a homemade electrolytic cell.

### Synthesis of PANI/CdS Heterojunction Nanowire Arrays.

First, a layer of Au was evaporated on one side of the AAO template as a conducting layer, and then the AAO template was put into a homemade electrolytic cell as a working electrode with a platinum counter electrode and a saturated calomel electrode (SCE) reference electrode. PANI deposition was carried out from a mixture of 0.2 M aniline and 0.5 M sulfuric acid aqueous solution by applying a voltage of 0.75 V (vs SCE) for an appropriate time (typically 750 s). Then, the AAO template containing PANI nanowires was used as a working electrode. CdS nanowires were deposited into the AAO template at a current density of 2.5  $\text{mA}/\text{cm}^2$  in a DMSO solution consisting of 0.055 M  $\text{CdCl}_2$  and 0.19 M elemental sulfur at 110  $^\circ\text{C}$ ; then the template was washed with hot DMSO and acetone. Finally, the PANI/CdS heterojunction nanowires embedded in an AAO membrane were obtained. The AAO template was selectively etched by NaOH solution (2 M) and cleaned by deionized water for later analysis.

**Preparation of PANI/CdS Heterojunction Nanowire Array Devices.** In general, the as prepared PANI/CdS heterojunction nanowire arrays were embedded in an AAO template; then the template was removed partly. The PANI/CdS heterojunction nanowire array film (the square area of the film was about 2  $\text{mm}^2$ ) was put on a Pt sheet and covered with an ITO on the top of the film. It was ensured that the Pt sheet and ITO were separated completely in the experiment. All of the

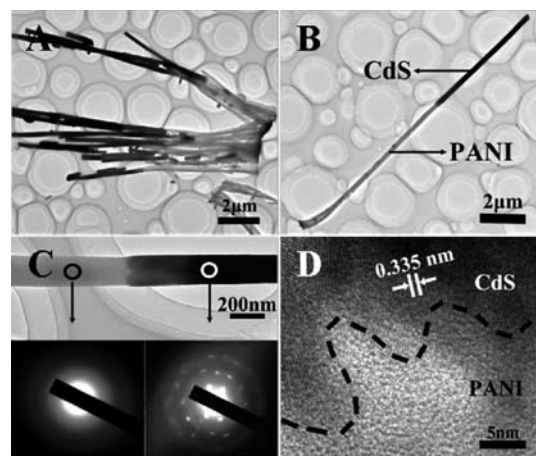


**Figure 2.** TEM images of PANI/CdS heterojunction nanowires. (A) PANI/CdS heterojunction nanowires. (B) A typical single PANI/CdS heterojunction nanowire. (C) Interface of PANI/CdS heterojunction nanowire under a higher magnification; the insets are SAED patterns taken from segments in the single PANI/CdS heterojunction nanowire. (D) HRTEM image of the interface of the PANI/CdS heterojunction nanowire.

devices measured in our experiment were made in a top-contact device configuration.

**Characterization.** Field emission scanning electron microscopy (SEM) and energy-dispersive X-microanalysis spectrum (EDS) patterns were taken from a JEOL JSM 4800F FESEM microscope at an accelerating voltage of 15 kV. The transmission electron microscopy (TEM), high resolution transmission electron microscopy (HRTEM) measurements, and selective-area electron diffraction patterns (SAED) were taken with a JEOL 2011 transmission electron microscope at an accelerating voltage of 200 kV. Confocal laser scanning microscopy (CLSM) images were acquired with a WITec CMR200 in the confocal Raman spectra mode. UV–visible absorption spectra were measured at room temperature with a Jasco V-570 spectrophotometer. Current–voltage ( $I$ – $V$ ) characteristics of devices were recorded with a Keithley 4200 SCS at room temperature in the air.

## RESULTS AND DISCUSSION

We used ordered porous AAO templates and chose the p-type organic semiconductor of PANI (polyaniline) and n-type inorganic semiconductor of CdS to prepare heterojunction nanowires according to a previous report.<sup>7</sup> The synthesis procedure is shown in Scheme S1 (see the Supporting Information). The morphologies and size of the PANI/CdS heterojunction nanowire arrays are characterized by SEM. Figure 1A revealed that nanowire arrays with the same length were prepared after the template was dissolved. These nanowires are well-defined, with a smooth surface and with diameters of about 200 nm. Figure 1B shows some typical heterojunction nanowires of PANI/CdS with a clear interface between organic and inorganic semiconductors. The EDS patterns (Figure S3A–C, Supporting Information) confirmed that the heterojunction nanowire was composed of PANI and CdS. The segmented structure of the PANI/CdS heterojunction nanowire can also be confirmed by CLSM (Figure 1C,D). The part with red fluorescence in the single PANI/CdS nanowire is the CdS segment, because its surface-trap emission ranged from 570 to 670 nm under excitation of 330–380 nm.<sup>29</sup> The dark part corresponds to PANI because PANI does not exhibit any fluorescence. Figure 1E and F show

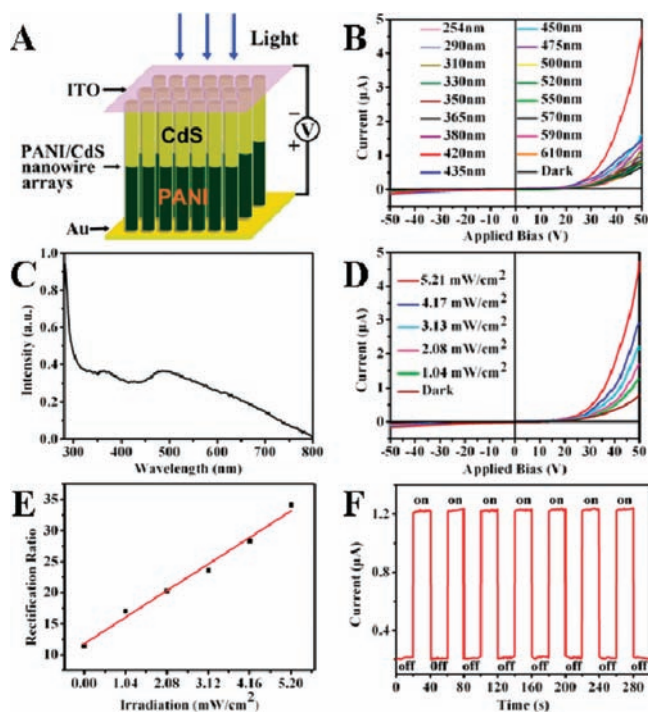


**Figure 3.** (A) Working model of PANI/CdS heterojunction nanowire array device. (B) Typical  $I$ – $V$  curves of PANI/CdS heterojunction nanowire arrays in dark and under illumination of different wavelength light. (C) Normalized UV–visible absorption spectra of PANI/CdS heterojunction nanowires suspended in ethanol. (D) Typical  $I$ – $V$  curves of PANI/CdS heterojunction nanowire arrays in the dark and under 420 nm light illumination. (E) Irradiance dependence of the rectification ratio of PANI/CdS heterojunction nanowire arrays in the dark and under 420 nm light illumination. (F) On/off switching of PANI/CdS heterojunction nanowire arrays upon pulsed illumination from 420 nm wavelength light with a power density of 5.21 mW/cm<sup>2</sup>.

the fluorescent images of some typical PANI/CdS heterojunction nanowires under excitation of 405 nm. The blue fluorescence and red fluorescence came from the band gap and surface-trap emission of the CdS segment, respectively. Further structure characterizations of the PANI/CdS heterojunction nanowires were performed using TEM and HRTEM, as shown in Figure 2. Figure 2A depicts some typical PANI/CdS heterojunction nanowires with a smooth surface. Figure 2B shows a typical single PANI/CdS heterojunction nanowire with a diameter about 200 nm. The heterojunction formed by CdS and PANI can be clearly observed. Figure 2C displays the interface of an independent heterojunction nanowire under a higher magnification, and the SAED of different segments in the nanowire shows that the bright part is amorphous PANI and the dark part is crystalline CdS. The HRTEM image (Figure 2D) reveals the exact interface structure of the PANI/CdS heterojunction nanowire, indicating the polycrystalline CdS attached firmly with amorphous PANI.

The electrical properties of p–n heterojunction nanowire arrays were investigated by measurements of the current ( $I$ ) versus bias voltage ( $V$ ). The devices were fabricated as described in Figure 3A. The typical  $I$ – $V$  curves of the independent PANI nanowire arrays in the dark exhibit that the PANI served as a semiconductor with a conductivity of about  $4 \times 10^{-6}$  S/cm (Figure S5A, Supporting Information). The  $I$ – $V$  curves of independent CdS

nanowire arrays show that the conductivity of CdS nanowire arrays in the dark is  $2.6 \times 10^{-6}$  S/cm, and the photoresponse was detected along with the increase in illumination intensity (Figure S5B, Supporting Information).

Figure 3B shows the typical  $I$ – $V$  curves obtained when PANI/CdS heterojunction nanowire arrays are exposed to light with different wavelengths. The current of PANI/CdS heterojunction nanowire arrays in the dark is very low. For the forward bias, the current increases as the applied voltage is incremented simultaneously. In reverse bias, the current transporting through the heterojunction of nanowire arrays is low. The PANI/CdS heterojunction nanowire arrays exhibit the remarkable performance of a light-controlled diode. Interestingly, under the illumination of different wavelengths of light, the conductivity of the PANI/CdS heterojunction nanowire arrays increased obviously. It can be seen that the current of the PANI/CdS heterojunction nanowire arrays is highest for the 420 nm wavelength light, and that for the other wavelengths of light was rather low. From the spectral response of PANI/CdS heterojunction nanowire arrays (Figure S4, Supporting Information), the rectification ratio of the PANI/CdS heterojunction nanowire array device reaches a maximum at 420 nm. The rectification ratio (RR) at the applied voltage  $V_0$  (50 V) is defined as  $RR = [\text{current at } V_0] / [\text{current at } -V_0]$ .<sup>30,31</sup> To clarify the origin of spectral response, the UV–visible absorption spectra of PANI/CdS heterojunction nanowires was measured, which is shown in Figure 3C. The enhancement of the photoconductive sensitivity is possibly due to the electron–hole pairs excited by the incident light with energy larger than the band gap; i.e., only light with enough photon energy is able to induce a significant increase in conductance. Light with less energy is not enough to excite electrons from the valence band to the conduction band and thus contributes little to the photocurrent. The slight increase of photosensitivity on the long wavelength side is possibly due to the transition of carriers from defect states in the band gap to the conduction band. The drop of sensitivity on the shorter wavelength side, which was also observed in the CdS film devices,<sup>32</sup> is attributed to the enhanced absorption of high energy photons at or near the surface region of the semiconductor. The electron–hole pairs generated near the surface region typically have a lifetime shorter than those in the bulk; hence they contribute less to the photoconductance.<sup>33</sup> Moreover, the photoresponse of PANI/CdS heterojunction nanowire arrays under an illumination intensity of 420 nm was also investigated. We observed the unique phenomenon of a light-controlled diode on the PANI/CdS heterojunction nanowire arrays. As shown in Figure 3D, with the increase of illumination intensity from dark to 5.21 mW/cm<sup>2</sup>, the rectification ratio of the PANI/CdS heterojunction nanowire arrays increased. Under the dark conditions, the rectification ratio of the diode is 11. With an increase in the illumination intensity (1.04 mW/cm<sup>2</sup>, 2.08 mW/cm<sup>2</sup>, 3.13 mW/cm<sup>2</sup>, 4.17 mW/cm<sup>2</sup>, 5.21 mW/cm<sup>2</sup>), the corresponding rectification ratio of the diode increased from 11.4, 17.0, 20.2, 23.6, 28.3, to 34.1. Photosensitivity is conveniently defined as the ratio of photoconductivity to dark conductivity, that is, photosensitivity = dark resistance/ photoresistance.<sup>32</sup> Using this equation, the photosensitivity of the PANI/CdS heterojunction nanowire arrays is 11.6. As depicted in Figure 3E, the rectification ratio plots of different illumination intensities show a straight line. A simple linear equation as given below can be applied to describe the relation of the rectification ratio ( $R$ ) and illumination intensity ( $E$ ), which is  $R = 4.13E + 11.67$ . Using this equation, illumination intensity

(*E*) can be calculated according to the rectification ratio (*R*) value. This means that illumination intensity can be quantitatively determined. An energy level diagram of the PANI/CdS heterojunction nanowire array device is shown in Figure S6 (Supporting Information), which shows that the diode nature originates from the integration of PANI and CdS. As expected, the PANI/CdS heterojunction nanowire arrays act as a diode and exhibit excellent rectifying properties under blue light illumination (420 nm) at room temperature, and illumination intensity can be quantitatively determined according to the rectification ratio. These characters are suitable as blue light photodetectors and key materials applied on the optoelectronic devices.

Repeatability and response speed are the key parameters which determine the capability of a photodetector to follow a quickly varying optical signal. Figure 3F shows the on/off switching of PANI/CdS heterojunction nanowire arrays at an incident light wavelength of 420 nm. The current was monitored at a bias of 20 V, while 420 nm wavelength light with a power density of 5.21 mW/cm<sup>2</sup> was turned on and off repeatedly for several cycles. With the light irradiation on and off, the current in the devices showed two distinct states, a “low” current in the dark and a “high” current under illumination. In the dark, the current was only 0.21 μA. However, under an incident light density of 5.21 mW/cm<sup>2</sup>, the current reaches 1.23 μA, giving an on/off switching ratio of about 5.8. When the light irradiation was turned off, the current decreased to the initial value. The switching in the two states reveals that the response of PANI/CdS heterojunction nanowire arrays to incident light (420 nm) is very fast and shows excellent stability and repeatability as well. Several unique characteristics of PANI/CdS heterojunction nanowire arrays are believed to contribute to the high response speed: (1) The first is the superior crystal quality of CdS nanowires. The density of traps induced by defects is drastically reduced; thus the photocurrent reaches a steady state rapidly in both the rise and decay stages. (2) The second is the high surface-to-volume ratio of PANI/CdS heterojunction nanowires. The defects and dangling bonds on the surface possibly serve as recombination centers, which would enhance the recombination of free carriers and shorten the decay time. (3) The final is a reduction of the recombination barrier in nanostructures.<sup>34</sup> Band bending usually occurs at the surface of semiconductors due to Fermi-level pinning, which leads to an energy barrier for recombination of electron–hole pairs.<sup>33</sup>

## CONCLUSIONS

In summary, we have designed and fabricated a blue light photodetector based on the PANI/CdS heterojunction nanowire arrays with unique properties. The as-prepared inorganic/organic p–n heterojunction nanowire arrays are well-defined and highly ordered and exhibit light-controlled diode performance and excellent rectifying features. Importantly, the inorganic/organic p–n heterojunction nanowire arrays show a sensitive spectral response and a significant response speed to blue light (420 nm), and the rectification ratio plots of different illumination intensities show straight line behavior, implying that a quantitative detection of illumination intensity can be achieved. With the light illumination on and off, the rectification ratio of the PANI/CdS heterojunction nanowire array device could respond quickly at “high” and “low” states with an “ON/OFF” ratio of about 11.6, and the device exhibits good stability and repeatability. The research results suggest great application potential

of the PANI/CdS heterojunction nanowire arrays for high-sensitivity and high-speed nanoscale photodetectors and photoelectronic switches.

## ASSOCIATED CONTENT

**S Supporting Information.** The synthesis procedure of PANI/CdS heterojunction nanowire arrays; SEM images of individual nanowires and nanowire arrays; the element mapping, linear scanning, and EDS patterns of the PANI/CdS heterojunction nanowire; typical *I*–*V* curves of PANI nanowire arrays and CdS nanowire arrays; and an energy level diagram. This material is available free of charge via the Internet at <http://pubs.acs.org>.

## AUTHOR INFORMATION

### Corresponding Author

\*Fax: +86-10-826-165-76. E-mail: [ylli@iccas.ac.cn](mailto:ylli@iccas.ac.cn); [liuhb@iccas.ac.cn](mailto:liuhb@iccas.ac.cn).

## ACKNOWLEDGMENT

This work was supported by the National Nature Science Foundation of China (21031006, 20831160507, 20873155, 10874187, and 90922007) and the National Basic Research 973 Program of China (2011CB932300).

## REFERENCES

- (1) Duan, X. F.; Huang, Y.; Cui, Y.; Wang, J. F.; Lieber, C. M. *Nature* **2001**, *409*, 66.
- (2) Liu, H. B.; Xu, J. L.; Li, Y. J.; Li, Y. L. *Acc. Chem. Res.* **2010**, *43*, 11496.
- (3) Garnett, E. C.; Yang, P. D. *J. Am. Chem. Soc.* **2008**, *130*, 9224.
- (4) Zhang, Y. J.; Dong, H. L.; Tang, Q. X.; Ferdous, S.; Liu, F.; Mannsfeld, S. C. B.; Hu, W. P.; Briseno, A. L. *J. Am. Chem. Soc.* **2010**, *132*, 11580.
- (5) Liu, X. F.; Li, Y. L. *Dalton Trans.* **2009**, 6447.
- (6) Huang, Y.; Duan, X. F.; Lieber, C. M. *Small* **2005**, *1*, 142.
- (7) Guo, Y. B.; Tang, Q. X.; Liu, H. B.; Zhang, Y. J.; Li, Y. L.; Hu, W. P.; Wang, S.; Zhu, D. B. *J. Am. Chem. Soc.* **2008**, *130*, 9198.
- (8) Guo, Y. B.; Zhang, Y. J.; Liu, H. B.; Lai, S. W.; Li, Y. L.; Li, Y. J.; Hu, W. P.; Wang, S.; Che, C. M.; Zhu, D. B. *J. Phys. Chem. Lett.* **2010**, *1*, 327.
- (9) Guo, Y. B.; Liu, H. B.; Li, Y. J.; Li, G. X.; Zhao, Y. J.; Song, Y. L.; Li, Y. L. *J. Phys. Chem. C* **2009**, *113*, 12669.
- (10) Liu, H. B.; Cui, S.; Guo, Y. B.; Li, Y. L.; Huang, C. S.; Zuo, Z. C.; Yin, X. D.; Song, Y. L.; Zhu, D. B. *J. Mater. Chem.* **2009**, *19*, 1031.
- (11) Briseno, A. L.; Holcombe, T. W.; Boukai, A. I.; Garnett, E. C.; Shelton, S. W.; Fréchet, J. M. J.; Yang, P. D. *Nano Lett.* **2010**, *10*, 334.
- (12) Hwang, Y. J.; Boukai, A.; Yang, P. D. *Nano Lett.* **2009**, *9*, 410.
- (13) Dong, Y. J.; Tian, B. Z.; Kempa, T. J.; Lieber, C. M. *Nano Lett.* **2009**, *9*, 2183.
- (14) Kind, H.; Yan, H. Q.; Messer, B.; Law, M.; Yang, P. D. *Adv. Mater.* **2002**, *14*, 158.
- (15) Sargent, E. H. *Adv. Mater.* **2005**, *17*, 515.
- (16) Gong, X.; Tong, M. H.; Xia, Y. J.; Cai, W. Z.; Moon, J. S.; Cao, Y.; Yu, G.; Shieh, C. L.; Nilsson, B.; Heeger, A. J. *Science* **2009**, *325*, 1665.
- (17) Wu, H.; Sun, Y.; Lin, D. D.; Zhang, R.; Zhang, C.; Pan, W. *Adv. Mater.* **2009**, *21*, 227.
- (18) Jiang, Y.; Zhang, W. J.; Jie, J. S.; Meng, X. M.; Fan, X.; Lee, S. T. *Adv. Funct. Mater.* **2007**, *17*, 1795.
- (19) Li, L.; Lee, P. S.; Yan, C. Y.; Zhai, T. Y.; Fang, X. S.; Liao, M. Y.; Koide, Y.; Bando, Y.; Golberg, D. *Adv. Mater.* **2010**, *22*, 1545.
- (20) Jin, Y. Z.; Wang, J. P.; Sun, B. Q.; Blakesley, J. C.; Greenham, N. C. *Nano Lett.* **2008**, *8*, 1649.

- (21) Wang, J. F.; Gudiksen, M. S.; Duan, X. F.; Cui, Y.; Lieber, C. M. *Science* **2001**, 293, 1455.
- (22) Freitag, M.; Martin, Y.; Misewich, J. A.; Martel, R.; Avouris, P. *Nano Lett.* **2003**, 3, 1067.
- (23) Wang, J. J.; Wang, Y. Q.; Cao, F. F.; Guo, Y. G.; Wan, L. J. *J. Am. Chem. Soc.* **2010**, 132, 12218.
- (24) Wang, J. J.; Cao, F. F.; Jiang, L.; Guo, Y. G.; Hu, W. P.; Wan, L. J. *J. Am. Chem. Soc.* **2009**, 131, 15602.
- (25) Amos, F. F.; Morin, S. A.; Streifer, J. A.; Hamers, R. J.; Jin, S. *J. Am. Chem. Soc.* **2007**, 129, 14296.
- (26) O'Brien, G. A.; Quinn, A. J.; Tanner, D. A.; Redmond, G. *Adv. Mater.* **2006**, 18, 2379.
- (27) Li, L.; Wu, P. C.; Fang, X. S.; Zhai, T. Y.; Dai, L.; Liao, M. Y.; Koide, Y.; Wang, H. Q.; Bando, Y.; Golberg, D. *Adv. Mater.* **2010**, 29, 3161.
- (28) Zhai, T. Y.; Li, L.; Wang, X.; Fang, X. S.; Bando, Y.; Golberg, D. *Adv. Funct. Mater.* **2010**, 20, 4233.
- (29) Cao, Y. C.; Wang, J. *J. Am. Chem. Soc.* **2004**, 126, 14336.
- (30) Manna, S.; Ashok, v. D.; De, S. K. *Appl. Mater. Interfaces* **2010**, 2, 3539.
- (31) Zhao, J. C.; Yu, C.; Wang, N.; Liu, H. M. *J. Phys. Chem. C* **2010**, 114, 4135.
- (32) Amalnerkar, D. P. *Mater. Chem. Phys.* **1999**, 60, 1.
- (33) Jie, J. S.; Zhang, W. J.; Jiang, Y.; Meng, X. M.; Li, Y. Q.; Lee, S. T. *Nano Lett.* **2006**, 6, 1887.
- (34) Calarco, R.; Marso, M.; Richter, T.; Aykanat, A. I.; Meijers, R.; Hart, A.; Stoica, T.; Lüth, H. *Nano Lett.* **2005**, 5, 981.